

# EEGNet: A Compact Convolutional Network for EEG-based Brain-Computer Interfaces

Vernon J. Lawhern<sup>1,2</sup>, Amelia J. Solon<sup>1,3</sup>, Nicholas R. Waytowich<sup>1,4</sup>, Stephen M. Gordon<sup>1,3</sup>,  
Chou P. Hung<sup>1,5</sup>, and Brent J. Lance<sup>1</sup>

<sup>1</sup>Human Research and Engineering Directorate, U.S. Army Research Laboratory, Aberdeen Proving Ground, MD

<sup>2</sup>Department of Computer Science, University of Texas at San Antonio, San Antonio, TX

<sup>3</sup>DCS Corporation, Alexandria, VA

<sup>4</sup>Department of Biomedical Engineering, Columbia University, New York, NY

<sup>5</sup>Department of Neuroscience, Georgetown University Medical Center, Washington, DC

May 10, 2017

## Abstract

*Objective:* Brain-Computer Interface (BCI) technologies enable direct communication between humans and computers by analyzing brain measurements, such as electroencephalography (EEG). BCI processing typically consists of heuristically extracting features for specific tasks, limiting the generalizability of the BCI across tasks. Here, we asked whether we can find a single generalized neural network architecture that can accurately classify EEG signals in different BCI tasks. *Approach:* In this work we introduce EEGNet, a compact fully convolutional network for EEG-based BCIs. We compare EEGNet to the current state-of-the-art approach across four different BCI classification tasks: P300 visual-evoked potentials, error-related negativity responses (ERN), movement-related cortical potentials (MRCP), and sensory motor rhythms (SMR). We fit 12 different architectures, all with the same number of parameters, to statistically control for the effect of model size versus model performance. *Results:* We show that one particular architecture performed on average the best over all datasets, suggesting that a generic model can be used for a variety of BCIs. We also show that EEGNet compares favorably to the current best state-of-the-art approach for each dataset across all four datasets. *Significance:* Our findings suggest that a common simplified architecture, EEGNet, can provide robust performance across many different BCI modalities.

## 1 Introduction

A Brain-Computer Interface (BCI) is a mechanism for communicating with a machine via brain signals, bypassing normal neuromuscular outputs [1]. Traditionally, BCIs, which have leveraged both invasive and noninvasive recording methods, have been used for medical applications such as neural control of prosthetic artificial limbs [2]. However, recent research has opened up the possibility for novel BCIs focused on enhancing performance of healthy users, often with noninvasive approaches based on electroencephalography (EEG). Generally speaking, a BCI consists of five main

processing stages [3]: a data collection stage, where neural data is recorded; a signal processing stage, where the recorded data is preprocessed and cleaned; a feature extraction stage, where meaningful information is extracted from the neural data; a classification stage, where a decision is interpreted from the data; and a feedback stage, where the result of that decision is provided to the user. While these stages are largely the same across BCI paradigms, each paradigm relies on manually specified methods for signal processing [4], feature extraction [5] and classification [6], a process which often requires significant subject-matter expertise and/or *a priori* knowledge about the expected EEG signal. It is also possible that, because the EEG signal preprocessing steps are often very specific to the EEG feature of interest (for example, band-pass filtering to a specific frequency range), other potentially relevant EEG features are being excluded from analysis (for example, features outside of the band-pass frequency range). The need for robust feature extraction will only continue to increase as BCI technologies evolve into new application domains [7–12].

*Deep Learning* has largely alleviated the need for manual feature extraction, achieving state-of-the-art performance in fields such as computer vision and speech recognition [13, 14]. The use of convolutional neural networks (CNNs) in particular has increased significantly, due in part to their success in many challenging image classification problems [14–18], surpassing methods that have relied on the use of hand-crafted features (see [19] and [20] for recent reviews). The majority of BCI systems, however, still rely on the use of handcrafted features. This raises the following question: Can Deep Learning approaches be used to design better features suitable for classification of EEG signals? While there have been many previous works on applying Deep Learning approaches to EEG signals (for example, epilepsy prediction and monitoring [21–25], sleep stage detection [26], anomaly detection [27], mental workload classification [28], auditory music retrieval [29, 30], detection of visual-evoked responses [31–34], control of exoskeletons [35] and motor imagery [36–38]), they were each optimized on a single BCI task, making it unclear how these approaches would generalize to other datasets.

In this work, we introduce *EEGNet*, a compact fully convolutional network capable of state-of-the-art performance across multiple BCI tasks. We evaluate offline model performance on four BCI tasks: P300 visual-evoked potential (P300), error-related negativity (ERN), movement-related cortical potential (MRCP) and the sensory motor rhythm (SMR). On these tasks, we systematically evaluate 12 variants of the EEGNet model architecture (defined as the configuration of each layer) while controlling for model size (defined as the total number of free parameters). Our model comparison analysis showed that one particular architecture performed on average the best over all four datasets, suggesting a generic configuration suitable for a variety of EEG-based BCIs. We also show that this architecture performs comparably to that of the current state-of-the-art approach for each of the four datasets.

## 2 Background

BCIs are generally categorized into two types, depending on the EEG feature of interest [39]: event-related and oscillatory. *Event-Related Potential* (ERP) BCIs are designed to detect an EEG response to a known, time-locked external stimulus. They are generally robust across subjects and contain well-stereotyped waveforms, enabling the exact time course of the ERP to be modeled through machine learning efficiently [40]. BCI systems can also leverage desynchronization/synchronization of EEG oscillations, such as those which might occur during a self-paced mental task or a change in user mental state. In contrast to ERP-based BCIs, which rely mainly on

the detection of the ERP waveform from some external event or stimulus, *Oscillatory* BCIs use the signal power of specific EEG frequency bands for external control and are generally not time-locked to an external stimulus [41]. When oscillatory signals are time-locked to an external stimulus, they can be represented through event-related spectral perturbation (ERSP) analyses [42]. Oscillatory BCIs are more difficult to train, generally due to the lower SNR as well as greater variation across subjects [41]. Oscillatory BCIs are also more susceptible to external noise sources when compared to ERP BCIs, and thus require more data and/or more advanced signal processing approaches to design effective systems [39].

## 2.1 Datasets

### 2.1.1 Dataset 1: P300 Event-Related Potential (P300)

The P300 event-related potential is a stereotyped neural response to novel visual stimuli [43]. It is most commonly elicited with the visual oddball paradigm, where participants are shown repetitive “nontarget” visual stimuli that are interspersed with infrequent “target” stimuli at a fixed presentation rate (for example, 1 Hz). Observed over the parietal cortex, the P300 waveform is a large positive deflection of electrical activity observed approximately 300 ms post stimulus onset, the strength of the observed deflection being inversely proportional to the frequency of observed targets. The P300 ERP is one of the strongest neural signatures observable by EEG, especially when targets are presented infrequently [43]. When the image presentation rate increases to 2 Hz or more, it is commonly referred to as rapid serial visual presentation (RSVP), which has been used to develop BCIs for large image database triage [44–46].

The EEG data used here were previously described in [45]; a brief description is given below. 18 participants volunteered for an RSVP BCI study. Participants were shown images of natural scenery at 2 Hz rate, with images either containing a vehicle or person (target), or with no vehicle or person present (nontarget). The target/nontarget ratio was 20%/80%. Data from 3 participants were excluded from the analysis due to excessive artifacts and/or noise within the EEG data. Data from the remaining 15 participants (9 male and 14 right-handed) who ranged in age from 18 to 57 years (mean age 39.5 years) were further analyzed. EEG recordings were digitally sampled at 512 Hz from 64 scalp electrodes arranged in a 10-10 montage using a BioSemi Active Two system (Amsterdam, The Netherlands). Continuous EEG data were referenced offline to the average of the left and right earlobes, digitally bandpass filtered to 1-40 Hz and downsampled to 128 Hz. Because of the class imbalance between target and nontarget trials, nontarget trials were randomly downsampled to match the number of target trials. EEG trials of target and nontarget conditions were extracted at  $[0, 1]$  seconds post stimulus onset, and used for a two-class classification.

### 2.1.2 Dataset 2: Feedback Error-Related Negativity (ERN)

Error potentials are perturbations of the EEG following an erroneous or unusual event in the subject’s environment or task. They can be observed in a variety of tasks, including time interval production paradigms [47] and in forced-choice paradigms [48, 49]. Here we focus on the feedback error-related negativity (ERN), which is an amplitude perturbation of the EEG following the perception of an erroneous feedback produced by a BCI. The feedback ERN is characterized as a large negative deflection approximately 300 ms after feedback, followed by a positive component 500 ms to 1 s after feedback (see Figure 7 of [50] for an illustration). The detection of the feedback ERN provides a mechanism to infer, and to possibly correct in real-time, the incorrect output of a BCI.

This two-stage system has been proposed as a hybrid BCI in [51,52] and has been shown to improve the performance of a P300 speller in online applications [53].

The EEG data used here come from [50] and were used in the “BCI Challenge” hosted by Kaggle (<https://www.kaggle.com/c/inria-bci-challenge>); a brief description is given below. 26 healthy participants (16 for training, 10 for testing) participated in a P300 speller task, a system which uses a random sequence of flashing letters, arranged in a  $6 \times 6$  grid, to elicit the P300 response [54]. The goal of the challenge was to determine whether the feedback of the P300 speller was correct or incorrect. The EEG data was originally recorded at 600 Hz using 56 passive Ag/AgCl EEG sensors (VSM-CTF compatible system) following the extended 10-20 system for electrode placement. Prior to our analysis, the EEG data was subsequently band-pass filtered to 1-40 Hz and down-sampled to 128 Hz. Because of the class imbalance between correct and incorrect feedback trials, correct feedback trials were randomly downselected to match the number of incorrect feedback trials. EEG trials of correct and incorrect feedback were extracted at  $[0, 1.25]$  seconds post feedback presentation and used as features for a two-class classification.

### 2.1.3 Dataset 3: Movement-Related Cortical Potential (MRCP)

Some neural activities contain both an ERP component as well as an oscillatory component. One particular example of this is the movement-related cortical potential (MRCP), which can be elicited by voluntary movements of the hands and feet and is observable through EEG along the central and midline electrodes, contralateral to the hand or foot movement [55]. The oscillatory component of the MRCP can be seen both before movement onset (an early desynchronization in the 10-12 Hz frequency band) as well as after movement onset (a late synchronization of 20-30 Hz activity approximately 1 s after movement execution). The ERP component of the MRCP occurs at the start of the movement, with a duration of approximately 800 ms. The MRCP has been used previously to develop motor control BCIs for both healthy and physically disabled patients [56].

The EEG data used here were previously described in [57]; a brief description is given below. In this study, 13 subjects performed self-paced finger movements using the left index, left middle, right index, or right middle fingers. This produced the well-known alpha and beta synchronizations (i.e. increases in power) and desynchronizations (i.e. decreases in power), most clearly observed over the contralateral motor cortex [58–60]. The data were originally recorded using a 256 channel BioSemi Active II system at 1024 Hz. Due to extensive signal noise present in the data, the EEG data were first processed with the PREP pipeline [61]. The data were referenced to linked mastoids, bandpass filtered between 1 Hz and 40 Hz, and then downsampled to 128 Hz. We further downsampled the channel space to the standard 64 channel BioSemi montage. The index and middle finger blocks for each hand were combined for binary classification of movements originating from the left or right hand. The classes are approximately balanced, with each subject having about 500 trials per class. EEG trials of left and right hand finger movements were extracted at  $[-.5, 1]$  seconds around finger movement onset and used for a two-class classification.

### 2.1.4 Dataset 4: Sensory Motor Rhythm (SMR)

A common control signal for oscillatory-based BCI is the sensorimotor rhythm (SMR), wherein  $\mu$  (8-12 Hz) and  $\beta$  (18-26 Hz) bands desynchronize over the sensorimotor cortex contralateral to an actual or imagined movement. The SMR is very similar to that of the oscillatory component of the MRCP. While SMR-based BCIs can facilitate nuanced, endogenous BCI control, they are not

Paradigm	Feature Type	# of Subjects	Trials per Subject	Train/Validation/Test Subjects
P300	ERP	15	~ 670	10/4/1
Feedback ERN	ERP	26	~ 200	12/4/10
MRCP	ERP/Oscillatory	13	~ 1100	8/4/1
SMR (BCI IV2A)	Oscillatory	9	288	8/1*/1*

Table 1: Summary of the data collections used in this study. For SMR we trained on all other subjects, used the test subjects’ training data as the validation set and tested on the subjects test set (see Section 2.2 for more details).

without their practical challenges. As signals, SMRs tend to be weak and highly variable across and within subjects, conventionally demanding user-training (neurofeedback) and long calibration times (20 minutes) in order to achieve reasonable performance [39].

The EEG data used here was Dataset 2A from BCI Competition IV [62] (called the SMR dataset for the remainder of the manuscript). The data consists of four classes of imagined movements of left and right hands, feet and tongue recorded from 9 subjects. The EEG data was originally recorded using 22 Ag/AgCl electrodes, sampled at 250 Hz and bandpass filtered between 0.5 and 100 Hz. Prior to our analysis we down-sampled the data to 128 Hz and refiltered with a bandpass filter between 4 and 40 Hz to minimize potential confounds due to low-frequency eye activity. For both the training and test sets we epoched the data at [0.5, 2.5] seconds post cue onset (the same window which was used in [38, 39]). Note that we make predictions for only this time range on the test set. We perform a four-class classification using accuracy as the summary measure.

## 2.2 EEG Data Processing

Table 1 has a summary of the four datasets. For the P300 and MRCP datasets, we randomly selected, without replacement, four subjects to be the validation set, one subject as the test set, and all remaining subjects in the training set. For the ERN dataset, the 10 test subjects we used here are the same as the subjects used in the Kaggle BCI competition. From the original 16 training subjects released as part of the competition, we selected four to be in the validation set and 12 to be in the training set. This process was repeated 30 times, producing 30 different folds. The mean and standard error of classification performance were calculated over the 30 folds.

For the SMR dataset, we constructed 9 folds as follows: For each subject, we set the training set to be the combination of training sets from all other subjects and set the current subjects training set to be the validation set. For example, for Subject 1, the training set would be the combined training sets from Subjects 2-9 and the validation set would be the training set from Subject 1. The test set remains the same as the original test set for the competition. This process repeats for each subject, creating 9 folds. The mean and standard error of classification performance were calculated over the 9 folds.

## 3 Methods

### 3.1 EEGNet Architecture

The EEGNet model is shown in Table 2, for EEG trials having  $C$  channels and  $T$  time samples. All layers used the Exponential Linear Unit (ELU) non-linear activation function [63] with parameter  $\alpha = 1$ . The model was estimated using Adam, a minibatch gradient descent algorithm using

Layer	Input ( $C \times T$ )	Operation	Output	Number of Parameters
1	$C \times T$	$16 \times \text{Conv1D} (C \times 1)$	$16 \times 1 \times T$	$16C + 16$
	$16 \times 1 \times T$	BatchNorm	$16 \times 1 \times T$	32
	$16 \times 1 \times T$	Transpose	$1 \times 16 \times T$	
	$1 \times 16 \times T$	Dropout (.25)	$1 \times 16 \times T$	
2	$1 \times 16 \times T$	$4 \times \text{Conv2D} (2 \times 32)$	$4 \times 16 \times T$	$4 \times 2 \times 32 + 4 = 260$
	$4 \times 16 \times T$	BatchNorm	$4 \times 16 \times T$	8
	$4 \times 16 \times T$	Maxpool2D (2,4)	$4 \times 8 \times T/4$	
	$4 \times 8 \times T/4$	Dropout (.25)	$4 \times 8 \times T/4$	
3	$4 \times 8 \times T/4$	$4 \times \text{Conv2D} (8 \times 4)$	$4 \times 8 \times T/4$	$4 \times 4 \times 8 \times 4 + 4 = 516$
	$4 \times 8 \times T/4$	BatchNorm	$4 \times 8 \times T/4$	8
	$4 \times 8 \times T/4$	Maxpool2D (2,4)	$4 \times 4 \times T/16$	
	$4 \times 4 \times T/16$	Dropout (.25)	$4 \times 4 \times T/16$	
4	$4 \times 4 \times T/16$	Softmax Regression	$N$	$TN + N$
Total				$16C + N(T + 1) + 840$

Table 2: EEGNet architecture, where  $C$  = number of channels,  $T$  = number of time points and  $N$  = number of classes, respectively. For Layers 1-3, the Exponential Linear Unit (ELU) activation function is used.

adaptive moment estimation [64], optimizing the categorical cross-entropy criterion, and running for 500 iterations (epochs). All models were trained on an NVIDIA Quadro K6000 GPU, with CUDA 7.5 and cuDNN v5, in Theano [65], using the Keras API [66].

- In Layer 1, we learn 16 convolutional kernels of size  $(C, 1)$ . This operation estimates a set of spatial filters over the entire period of the trial and is similar to that of previous approaches such as Common Spatial Patterns (CSP) [67], xDAWN spatial filtering [68] and independent component analysis (ICA) [69]. Note that these approaches are specifically designed to produce spatial filters that either maximize the variance difference among two classes (CSP), enhance the signal to signal-plus-noise ratio of the EEG signal of interest (xDAWN) or produce spatial filters that are as mutually independent as possible (ICA). In contrast, the spatial filters used here are optimized to minimize the cross-entropy of the predicted outputs and are therefore not required to achieve either optimal variance separation or mutual independence. The spatial filters are regularized with an elastic-net ( $L_1 + L_2$ ) constraint, with  $L_1 = 0.0001$  and  $L_2 = 0.0001$ . We apply Batch Normalization [70] together with Dropout [71] as this improved model robustness (See Appendix for more details). The output is transposed to produce a new 2 dimensional time series of shape (filters  $\times$  samples).
- In Layer 2, we learn 4 2-dimensional convolutional kernels of size  $(2 \times 32)$  on the output feature maps from Layer 1. 2D max-pooling is applied to the data; while this operation is traditionally done to induce invariance to image transformation in computer vision [72], we find that for processing EEG data this operation is beneficial primarily for dimension reduction. The total reduction in parameter size due to max-pooling is by a factor of 8 ( $2 \times 4$ ). As in Layer 1, Batch Normalization and Dropout are used.
- In Layer 3, we learn 4 2-dimensional convolutional kernels of size  $(8 \times 4)$ . All the operations in Layer 2 are also applied here.
- In Layer 4, the features are passed directly to a softmax classification with  $N$  units,  $N$  being the number of classes in the data. We omit the use of a dense layer for feature aggregation prior to the softmax classification layer to reduce the number of free parameters in the model, inspired in part by the work in [73] (see Appendix for more details).

### 3.2 Convolutional Network Model Comparison

In order to statistically separate the effects of model size (number of parameters) and model architecture versus classification performance, we generated 12 different models, all having the same number of parameters, using the model framework described in Table 2. We generated the 12 models by setting the convolutional kernel sizes in Layer 2 to be one of 4 different values: (16, 4), (8, 8), (4, 16) and (2, 32) and the kernel sizes in Layer 3 to be one of 3 different values: (8, 4), (4, 8) and (2, 16). Each architecture emphasizes different spatial/temporal aspects of the spatially-filtered EEG signal at different layers of the architecture.

### 3.3 Comparison with Shallow Approaches

We compare the performance of EEGNet to that of the best performing shallow reference algorithm for each individual paradigm. Here we use the term “shallow” to represent learning algorithms which are not multi-layer neural networks. For all ERP-based data analyses (P300, ERN, MRCP) the reference algorithm is the approach which won the Kaggle BCI Competition (code and documentation at <http://github.com/alexandrebarachant/bci-challenge-ner-2015>), which uses a combination of xDAWN Spatial Filtering [68], Riemannian Geometry [74, 75], channel subset selection and  $L_1$  feature regularization (referred to as xDAWN + RG for the remainder of the manuscript). While the original solution used an ensemble of classifiers using bagging, for this analysis we only compared a single model with this approach to a single EEGNet model on identical training and test sets, as we expect any gains from ensemble learning to benefit both approaches equally. We omit the use of both the Meta and Leak features for this analysis.

For oscillatory-based classification of SMR, the reference algorithm is the One-Versus-Rest (OVR) filter-bank common spatial pattern (FBCSP) algorithm as described in [76]. Note that the FBCSP classifiers in [76] were trained *within-subject*, while the EEGNet classifiers were trained *across-subject*.

### 3.4 Comparison with Deep Approaches

We also compare the performance of EEGNet to two recent convolutional networks for EEG. For all ERP-based analyses we compare EEGNet to the convolutional network model by Manor and Geva [32] (see Table 1 of [32]). Their work focused on the classification of P300 ERPs in a Rapid Serial Visual Presentation (RSVP) task. Their model consists of 3 convolutional layers (1 spatial, 2 temporal), 2 pooling layers and 2 fully connected layers. We fit their model to our data collections with some minor modifications. First, since their model was designed using EEG data sampled at 64 Hz, we appropriately scaled the length of the temporal kernels to match the rate of our data (128 Hz) to model the same amount of time temporally. Second, [32] uses Dropout after fully-connected layers, however the dropout fraction was not specified. Therefore, we set it to 0.5 for our comparison. Their model has approximately 11.8 million parameters for 1 second of EEG data at 128Hz, which represents more than a 5000-fold increase in parameter size when compared to EEGNet. This model will be referred to as the “MG” model for the remainder of the manuscript.

For the four-class classification task in the SMR dataset, we compare EEGNet to the Shallow ConvNet architecture recently proposed by [77]. Their architecture consists of two convolutional layers (temporal, then spatial), a squaring nonlinearity ( $f(x) = x^2$ ), an average pooling layer and a log nonlinearity ( $f(x) = \log(x)$ ) (see Figure 2 of [77] for an illustration). This architecture extracts features that closely resemble the trial log-bandpower features extracted by FBCSP, and

was shown to outperform FBCSP on BCI Competition 2A [77]. We modified the temporal kernels used in ShallowConvNet to match the sampling rate of our signal (250 Hz in the original architecture versus 128 Hz used here).

### 3.5 Effect of Training Set Size vs. Classification Performance

We also conducted an additional analysis where model performance was compared relative to the number of EEG trials in the training set, where from the full training set we randomly sampled, without replacement,  $K$  trials and set this random sample to be the training set. For all analyses we start with  $K = 500$  trials, then increase by 500 trials up to the total number of available trials. This procedure was repeated 10 times for each value of  $K$ . The mean and standard error of classification performance per training set size were calculated over the 10 repetitions.

### 3.6 Statistical Analysis

Statistically significant differences between the 12 EEGNet model configurations and the reference algorithm were tested using a nonparametric two-tailed sign-rank test for each model configuration, with a False Discovery Rate (FDR) correction [78] to control for multiple comparisons.

## 4 Results

Figure 1 shows the classification performance of the 12 EEGNet model configurations for each dataset, with the solid red line and shaded red region denoting the mean and two standard errors of the reference algorithm performance (xDAWN + RG for P300/ERN/MRCP and FBCSP for SMR), respectively. We observed minimal differences in performance of the 12 EEGNet models across the P300 and ERN datasets, while greater variation in performance was observed for SMR and in MRCP. For example, the  $[16, 4] \times [2, 16]$  model configuration, while performing the best on P300, was slightly worse in SMR and among the worst models for MRCP. When we ranked the 12 EEGNet models in descending order per dataset (so the 1<sup>st</sup> model performed the best and 12<sup>th</sup> model performed the worst) and averaged over the 4 datasets, we found that the  $[2, 32] \times [8, 4]$  model configuration seemed to perform the best overall (Table 3), although it is difficult to determine statistical significance, given only four data points per model configuration. We also found that models with 2<sup>nd</sup> and 3<sup>rd</sup> layers that iterated either between spatial and temporal (or vice-versa) tended to perform better than models that only focused on spatial or temporal aspects of the data in both layers. The EEGNet model with the  $[2, 32] \times [8, 4]$  configuration will be used for the remainder of the manuscript.

Across the three ERP-based datasets (P300, ERN, MRCP) we found that EEGNet outperformed xDAWN + RG for P300 (approx. 0.05 AUC improvement,  $p < 0.05$ ), performed about the same in MRCP (approx. 0.01 AUC improvement,  $p > 0.05$ ), and performed slightly worse in ERN (approx. 0.02 AUC decrease,  $p < 0.05$ ). Note that the hyperparameters for xDAWN + RG, such as the number of xDAWN spatial filters to calculate per class (5) and the number of down-selected channels to use (35) were taken from the winning solution of the Kaggle BCI Competition (See Methods for more details). We also observed that EEGNet tends to produce predictions with slightly lower standard errors than xDAWN + RG for the three ERP datasets, suggesting tighter prediction performance. For the SMR dataset, we see that, on average, within-subject FBCSP



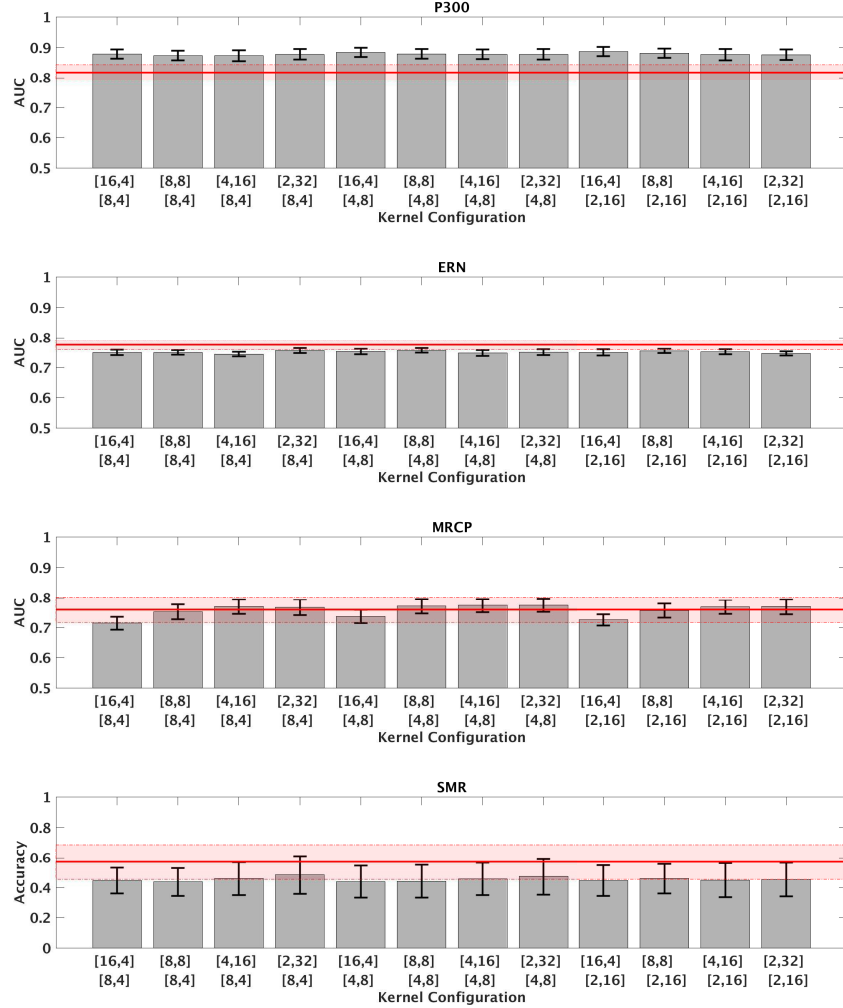


Figure 1: Classification performance for all 12 EEGNet models across all paradigms. The rows of the x-axis labels denote the  $2^{nd}$  and  $3^{rd}$  layer kernel configuration, respectively. Bars denotes the mean performance, averaged over 30 folds (9 for SMR), for each kernel configuration, while error bars denote 2 standard errors of the mean. The solid red line denotes the mean performance of the reference algorithm (xDAWN + RG for P300/ERN/MRCP and FBCSP for SMR), while the red shaded region denote two standard errors of the mean. All model configurations performed comparably with the shallow reference algorithm.

outperforms cross-subject EEGNet for all model configurations; when breaking down model performance per subject we observed significant performance differences across subjects (see Figure 2). In particular, we see that a cross-subject EEGNet performs within a few percentage points of FBCSP for some subjects (1, 8, 9), performs worse for a few other subjects (2, 4, 5) and outperforms FBCSP for two subjects (3, 6). We observed significant drops in EEGNet performance for Subject 7 when compared to FBCSP.

Figure 3 shows the classification performance in the ERP-based datasets based on the number of samples in the training set. EEGNet can outperform both xDAWN + RG and the MG model

Kernel		3 <sup>rd</sup> Layer		
Configuration		[8, 4]	[4, 8]	[2, 16]
2 <sup>nd</sup> Layer	[16, 4]	9.00 (1.47)	7.00 (2.38)	6.5 (2.06)
	[8, 8]	9.75 (0.75)	4.25 (1.31)	4.25 (1.25)
	[4, 16]	8.25 (2.17)	6.25 (1.65)	7.25 (1.03)
	[2, 32]	<b>3.75</b> (1.60)	4.25 (1.65)	7.50 (1.75)

Table 3: Rank of the 12 EEGNet model configurations, averaged over all four datasets (P300, ERN, MRCP, SMR). Numbers in parentheses denote the standard error of the mean. We see that the  $[2, 32] \times [8, 4]$  model ranks the best among all kernel configurations.

across all dataset sizes for the P300 dataset. We observed a significantly larger standard error for the MG model; this is due to the model failing to learn (0.5 AUC) for approximately 30% of the folds. For the ERN and MRCP datasets the MG model failed to learn across all folds and all training set sizes. We believe this is mainly due to the parameter size of the MG model, which contains approximately 11.8 million parameters. Given such small datasets used in this study, it is very difficult to learn a model of this size robustly. For the ERN dataset EEGNet performs similarly with xDAWN + RG up to 1500 training trials; at 2000 training trials xDAWN + RG begins to outperform EEGNet. The MRCP dataset has the largest difference between xDAWN + RG and EEGNet. xDAWN + RG begins to learn with just 500 training samples; performance starts to taper off after approximately 5000 trials. In contrast, EEGNet fails to learn a good classifier until at least 5000 trials are observed. Having more than 5000 trials increases performance significantly, approaching the performance of xDAWN + RG at 8000 trials. This trend suggests that EEGNet could potentially outperform xDAWN + RG given a larger dataset.

Figure 4 shows the same analysis as in Figure 3, but for Subject 1 from the SMR Dataset. Here we compare EEGNet to the ShallowConvNet architecture proposed in [77] (See Methods for more details) and to a within-subject FBCSP. We see that EEGNet outperforms the ShallowConvNet across all training set sizes, and approaches the performance of FBCSP at 1500 to 2000 training

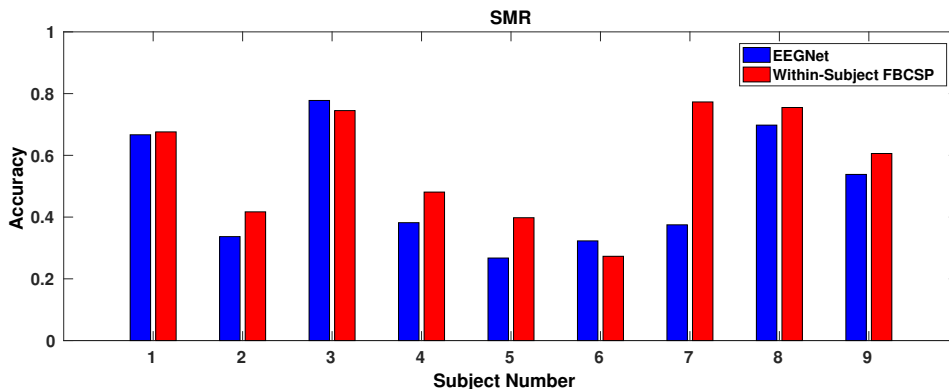


Figure 2: Classification performance of EEGNet versus within-subject FBCSP on the test data for the SMR dataset ( $n = 9$ ). Here, each bar denotes the test set performance per subject in the SMR dataset. EEGNet performed comparably with within-subject FBCSP across most subjects.

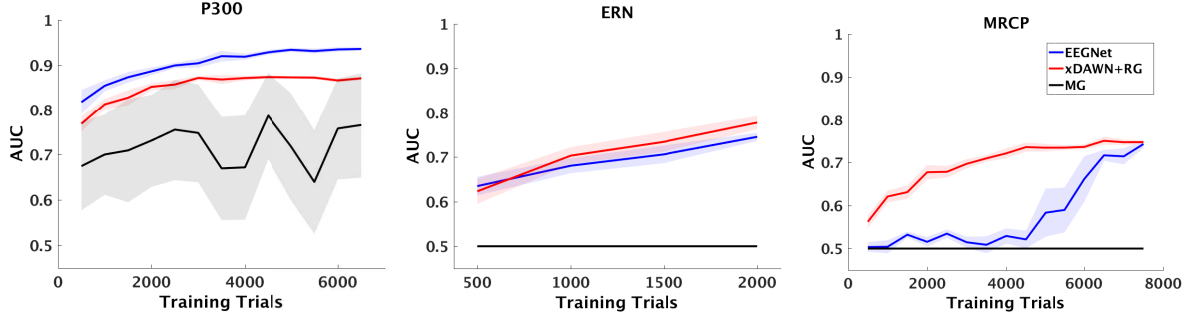


Figure 3: Difference in AUC performance of EEGNet when compared to both xDAWN + RG and the MG model for all ERP-based datasets (P300, ERN, MRCP) for one chosen fold. Solid lines denote the mean performance at each training set size, while shaded regions denote 2 standard errors of the mean. The MG model failed to converge for ERN and MRCP across all folds.

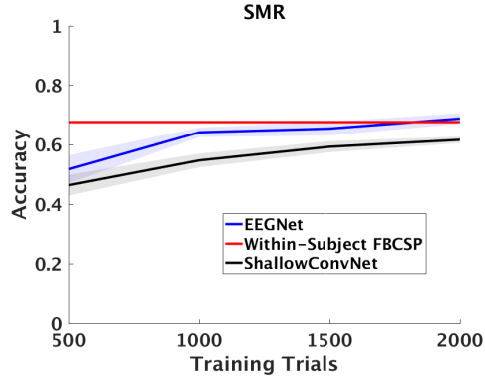


Figure 4: Difference in 4-class classification accuracy of EEGNet when compared to ShallowConvNet and the within-subject FBCSP performance for Subject 1 of the SMR dataset. The blue and black solid lines denote the mean classification performance of EEGNet and ShallowConvNet, respectively, across training set size. The shaded regions denote two standard errors of the mean. The solid red line denotes the One-Versus-Rest (OVR) within-subject FBCSP performance for Subject 1 as reported in [76].

trials.

## 5 Discussion

In this work we proposed *EEGNet*, a compact fully-convolutional network for EEG-based BCIs. We evaluated EEGNet against the state-of-the-art approach for both ERP and Oscillatory-based BCIs across four EEG datasets: P300 visual-evoked potentials, Error-Related Negativity (ERN), Movement-Related Cortical Potentials (MRCP) and Sensory Motor Rhythms (SMR). We showed that EEGNet can provide comparable performance in all four cases, with P300 classification providing a significant increase over the current best method (xDAWN + RG). To the best of our knowledge this represents the first work that has validated the use of a single network architecture against multiple BCIs, each with their own neural feature characteristics. This suggests that an

end-to-end system can be used for classification in EEG-based BCIs.

Across all four datasets, we observed minimal variability among the 12 EEGNet model configurations for the P300 and ERN, with larger amounts of variability for the MRCP and SMR datasets (see Figure 1). This performance difference coincides with the SNR of the signals of interest for each dataset. The P300 visual-evoked response is one of the strongest neural signatures observable from EEG [43], and thus the relevant features needed for classification can be captured by all 12 models fairly equally (the difference between the best and worse performing model on average is approximately 0.01 AUC). In contrast, the MRCP, as a neural signal, has very low SNR, requiring much more data and an appropriate model configuration to capture relevant features (see Figures 1 and 3). This generally holds true for the SMR signal as well, due to its inherent relationship with the MRCP signal.

Our model comparison analysis showed that a general model configuration can be used whenever knowledge of a particular EEG feature of interest is not known a priori (see Table 3). Because all the models have exactly the same number of parameters, statistically speaking the performance of the model can be primarily attributed to the kernel configuration itself. The model alternates between convolutions along spatial (Layers 1 and 3) and temporal (Layer 2) dimensions. This makes intuitive sense in terms of efficient model parametrization using filter factorization. For example, to represent an EEG segment of size  $[C, T]$ , for  $C$  channels and  $T$  time points, one could model the kernel size as  $[C, T]$  directly, incurring  $C \times T$  total parameters, or one could model the EEG segment with two layers, with the first layer having a kernel size of  $[C, 1]$  and the second layer having a kernel size of  $[1, T]$ , incurring a total of  $C + T$  parameters. It is easy to see that both approaches model the same segment of data; however, the second approach represents a significant reduction in the total number of parameters. This parametrization trick has been used by several groups [16, 17] as a way to efficiently build deep convolutional networks for image analysis. We essentially use the same strategy here to represent the EEG time series in a compact manner by aggregating information over the spatial and temporal dimensions iteratively. Another observation is that models whose 2<sup>nd</sup> and 3<sup>rd</sup> layer kernels emphasized only the spatial or temporal dimension (top left and bottom right corners of Table 3) performed on average worse than models that iterated between spatial and temporal dimensions (top right and bottom left corners of Table 3). This suggests that an iterative convolution scheme is important for extracting relevant features from EEG.

Deep Learning models for EEG generally employ one of three input styles, depending on their targeted application: (1) the EEG signal of all available channels, (2) a transformed EEG signal (generally a time-frequency decomposition) of all available channels [28] and (3) a transformed EEG signal of a subset of channels [36]. Models that fall in (2) generally see a significant increase in data dimensionality, thus requiring either more data or more model regularization (or both) to learn an effective feature representation. This introduces more hyperparameters that must be learned, increasing the potential variability in model performance due to hyperparameter misspecification. Models that fall in (3) generally require *a priori* knowledge about the channels to select. For example, the model proposed in [36] uses the time-frequency decomposition of channels Cz, C3 and C4 as the inputs for a motor imagery classification task. This channel selection is intentional, given the fact that neural responses to motor actions (the sensory motor rhythm) are observed strongest at those channels and are easily observed through a time-frequency analysis. Also, by only working with three channels, the authors mitigate the increase in dimensionality incurred by the time-frequency transformation. While this approach works well if the feature of interest is known beforehand, this approach is not guaranteed to work well in other applications where the

features are not observed at those channels, limiting overall utility. We believe models that fall in (1), such as EEGNet and others [31, 33, 34], offer the best tradeoff between input dimensionality and the flexibility to discover relevant features by providing all available channels. An additional advantage of EEGNet is its use of iterative spatial and temporal convolutions to extract relevant features, an aspect not commonly found in existing models for EEG. This is especially important as BCI technologies evolve into novel application spaces, such as BCIs for monitoring of mental states such as fatigue or stress [79], as the features needed for these BCIs may not be known beforehand.

The EEGNet model employs both Dropout regularization [71] and Batch Normalization [70]. While these operations have been used in other fields extensively to great success, it was unclear whether these operations would also be useful for EEG analysis. We tested several different model variations to determine the effects of these operations on each of the four datasets (See Appendix). We found that a model with both Dropout and Batch Normalization produced consistently lower validation losses across all four datasets than with Dropout and Batch Normalization separately. We believe that, given the low SNR of EEG together with traditionally small datasets, that these operations are necessary to learn the true underlying neural signal.

The first three layers of EEGNet can potentially be used as a preprocessing step prior to using recurrent neural networks for modeling long temporal sequences in the EEG. Recently, a recurrent convolutional network was proposed by [28] to predict mental workload. Their approach first used fourier transforms to convert the EEG time series into a time-frequency representation. This representation was then used in a recurrent neural network to model temporal dependencies in the time-frequency space. In our future work we will explore a similar approach, where we will replace the manually derived representation (time-frequency space) with the automatically-derived representation from the EEGNet model as the initial feature extraction, with the goal of analyzing non-time-locked EEG events.

## Acknowledgment

This project was sponsored by the U.S. Army Research Laboratory under CAST 076910227001, ARL-H70-HR52, ARL-74A-HRCYB and through Cooperative Agreement Number W911NF-10-2-0022. The views and conclusions contained in this document are those of the authors and should not be interpreted as representing the official policies, either expressed or implied, of the U.S. Government.

## References

- [1] J. R. Wolpaw, N. Birbaumer, D. J. McFarland, G. Pfurtscheller, and T. M. Vaughan, "Brain-computer interfaces for communication and control." *Clinical neurophysiology : official journal of the International Federation of Clinical Neurophysiology*, vol. 113, no. 6, pp. 767–91, jun 2002. [Online]. Available: <http://www.ncbi.nlm.nih.gov/pubmed/12048038>
- [2] A. B. Schwartz, X. T. Cui, D. Weber, and D. W. Moran, "Brain-controlled interfaces: Movement restoration with neural prosthetics," *Neuron*, vol. 52, no. 1, pp. 205 – 220, 2006.
- [3] L. F. Nicolas-Alonso and J. Gomez-Gil, "Brain computer interfaces, a review," *Sensors*, vol. 12, no. 2, p. 1211, 2012.
- [4] A. Bashashati, M. Fatourechi, R. K. Ward, and G. E. Birch, "A survey of signal processing algorithms in braincomputer interfaces based on electrical brain signals," *Journal of Neural Engineering*, vol. 4, no. 2, p. R32, 2007. [Online]. Available: <http://stacks.iop.org/1741-2552/4/i=2/a=R03>

- [5] D. J. McFarland, C. W. Anderson, K. R. Muller, A. Schlogl, and D. J. Krusienski, “Bci meeting 2005-workshop on bci signal processing: feature extraction and translation,” *IEEE Transactions on Neural Systems and Rehabilitation Engineering*, vol. 14, no. 2, pp. 135–138, June 2006.
- [6] F. Lotte, M. Congedo, A. Lcuyer, F. Lamarche, and B. Arnaldi, “A review of classification algorithms for eeg-based braincomputer interfaces,” *Journal of Neural Engineering*, vol. 4, no. 2, p. R1, 2007. [Online]. Available: <http://stacks.iop.org/1741-2552/4/i=2/a=R01>
- [7] T. O. Zander and C. Kothe, “Towards passive braincomputer interfaces: applying braincomputer interface technology to humanmachine systems in general,” *Journal of Neural Engineering*, vol. 8, no. 2, p. 025005, 2011. [Online]. Available: <http://stacks.iop.org/1741-2552/8/i=2/a=025005>
- [8] B. J. Lance, S. E. Kerick, A. J. Ries, K. S. Oie, and K. McDowell, “Brain-computer interface technologies in the coming decades,” *Proceedings of the IEEE*, vol. 100, no. Special Centennial Issue, pp. 1585–1599, May 2012.
- [9] S. Saproo, J. Faller, V. Shih, P. Sajda, N. R. Waytowich, A. Bohannon, V. J. Lawhern, B. J. Lance, and D. Jangraw, “Cortically coupled computing: A new paradigm for synergistic human-machine interaction,” *Computer*, vol. 49, no. 9, pp. 60–68, Sept 2016.
- [10] J. van Erp, F. Lotte, and M. Tangermann, “Brain-Computer Interfaces: Beyond Medical Applications,” *Computer*, vol. 45, no. 4, pp. 26–34, Apr. 2012.
- [11] B. Blankertz, M. Tangermann, C. Vidaurre, S. Fazli, C. Sannelli, S. Haufe, C. Maeder, L. E. Ramsey, I. Sturm, G. Curio, and K. R. Müller, “The berlin brain-computer interface: Non-medical uses of bci technology,” *Frontiers in Neuroscience*, vol. 4, no. 198, 2010.
- [12] S. M. Gordon, M. Jaswa, A. J. Solon, and V. J. Lawhern, “Real world bci: Cross-domain learning and practical applications,” in *Proceedings of the 2017 ACM Workshop on An Application-oriented Approach to BCI out of the Laboratory*, ser. BCIforReal ’17. New York, NY, USA: ACM, 2017, pp. 25–28. [Online]. Available: <http://doi.acm.org/10.1145/3038439.3038444>
- [13] G. Hinton, L. Deng, D. Yu, G. E. Dahl, A. r. Mohamed, N. Jaitly, A. Senior, V. Vanhoucke, P. Nguyen, T. N. Sainath, and B. Kingsbury, “Deep neural networks for acoustic modeling in speech recognition: The shared views of four research groups,” *IEEE Signal Processing Magazine*, vol. 29, no. 6, pp. 82–97, Nov 2012.
- [14] K. He, X. Zhang, S. Ren, and J. Sun, “Deep residual learning for image recognition,” *CoRR*, vol. abs/1512.03385, 2015. [Online]. Available: <http://arxiv.org/abs/1512.03385>
- [15] A. Krizhevsky, I. Sutskever, and G. E. Hinton, “Imagenet classification with deep convolutional neural networks,” in *Advances in Neural Information Processing Systems*, F. Pereira, C. J. C. Burges, L. Bottou, and K. Q. Weinberger, Eds., 2012, pp. 1097–1105. [Online]. Available: <http://papers.nips.cc/paper/4824-imagenet-classification-with-deep-convolutional-neural-networks.pdf>
- [16] K. Simonyan and A. Zisserman, “Very deep convolutional networks for large-scale image recognition,” *CoRR*, vol. abs/1409.1556, 2014. [Online]. Available: <http://arxiv.org/abs/1409.1556>
- [17] C. Szegedy, W. Liu, Y. Jia, P. Sermanet, S. E. Reed, D. Anguelov, D. Erhan, V. Vanhoucke, and A. Rabinovich, “Going deeper with convolutions,” *CoRR*, vol. abs/1409.4842, 2014. [Online]. Available: <http://arxiv.org/abs/1409.4842>
- [18] G. Huang, Z. Liu, K. Q. Weinberger, and L. van der Maaten, “Densely connected convolutional networks,” *CoRR*, vol. abs/1608.06993, 2016. [Online]. Available: <http://arxiv.org/abs/1608.06993>
- [19] Y. LeCun, Y. Bengio, and G. Hinton, “Deep learning,” *Nature*, vol. 521, pp. 436–444, 2015.
- [20] J. Schmidhuber, “Deep learning in neural networks: An overview,” *arXiv*, vol. abs/1404.7828, 2014. [Online]. Available: <http://arxiv.org/abs/1404.7828>
- [21] A. Antoniadis, L. Spyrou, C. C. Took, and S. Sanei, “Deep learning for epileptic intracranial eeg data,” in *2016 IEEE 26th International Workshop on Machine Learning for Signal Processing (MLSP)*, Sept 2016, pp. 1–6.
- [22] J. Liang, R. Lu, C. Zhang, and F. Wang, “Predicting seizures from electroencephalography recordings: A knowledge transfer strategy,” in *2016 IEEE International Conference on Healthcare Informatics (ICHI)*, Oct 2016, pp. 184–191.
- [23] A. Page, C. Shea, and T. Mohsenin, “Wearable seizure detection using convolutional neural networks with transfer learning,” in *2016 IEEE International Symposium on Circuits and Systems (ISCAS)*, May 2016, pp. 1086–1089.

- [24] P. Mirowski, D. Madhavan, Y. LeCun, and R. Kuzniecky, “Classification of patterns of {EEG} synchronization for seizure prediction,” *Clinical Neurophysiology*, vol. 120, no. 11, pp. 1927 – 1940, 2009.
- [25] P. Thodoroff, J. Pineau, and A. Lim, “Learning robust features using deep learning for automatic seizure detection,” *CoRR*, vol. abs/1608.00220, 2016. [Online]. Available: <http://arxiv.org/abs/1608.00220>
- [26] M. Långkvist, L. Karlsson, and A. Loutfi, “Sleep stage classification using unsupervised feature learning,” *Adv. Artif. Neu. Sys.*, vol. 2012, pp. 5:5–5:5, Jan. 2012. [Online]. Available: <http://dx.doi.org/10.1155/2012/107046>
- [27] D. F. Wulsin, J. R. Gupta, R. Mani, J. A. Blanco, and B. Litt, “Modeling electroencephalography waveforms with semi-supervised deep belief nets: fast classification and anomaly measurement,” *Journal of Neural Engineering*, vol. 8, no. 3, p. 036015, 2011.
- [28] P. Bashivan, I. Rish, M. Yeasin, and N. Codella, “Learning representations from EEG with deep recurrent-convolutional neural networks,” *CoRR*, vol. abs/1511.06448, 2015. [Online]. Available: <http://arxiv.org/abs/1511.06448>
- [29] S. Stober, D. J. Cameron, and J. A. Grahn, “Using convolutional neural networks to recognize rhythm stimuli from electroencephalography recordings,” in *Advances in Neural Information Processing Systems 27*, Z. Ghahramani, M. Welling, C. Cortes, N. D. Lawrence, and K. Q. Weinberger, Eds. Curran Associates, Inc., 2014, pp. 1449–1457.
- [30] S. Stober, A. Sternin, A. M. Owen, and J. A. Grahn, “Deep feature learning for EEG recordings,” *CoRR*, vol. abs/1511.04306, 2015. [Online]. Available: <http://arxiv.org/abs/1511.04306>
- [31] H. Cecotti and A. Graser, “Convolutional neural networks for p300 detection with application to brain-computer interfaces,” *IEEE Transactions on Pattern Analysis and Machine Intelligence*, vol. 33, no. 3, pp. 433–445, March 2011.
- [32] R. Manor and A. Geva, “Convolutional neural network for multi-category rapid serial visual presentation bci,” *Frontiers in Computational Neuroscience*, vol. 9, no. 146, 2015.
- [33] J. Shamwell, H. Lee, H. Kwon, A. R. Marathe, V. Lawhern, and W. Nothwang, “Single-trial eeg rsvp classification using convolutional neural networks,” pp. 983 622–983 622–10, 2016. [Online]. Available: <http://dx.doi.org/10.1117/12.2224172>
- [34] H. Cecotti, M. P. Eckstein, and B. Giesbrecht, “Single-trial classification of event-related potentials in rapid serial visual presentation tasks using supervised spatial filtering,” *IEEE Transactions on Neural Networks and Learning Systems*, vol. 25, no. 11, pp. 2030–2042, Nov 2014.
- [35] N.-S. Kwak, K.-R. Miller, and S.-W. Lee, “A convolutional neural network for steady state visual evoked potential classification under ambulatory environment,” *PLOS ONE*, vol. 12, no. 2, pp. 1–20, 02 2017. [Online]. Available: <http://dx.doi.org/10.1371/journal.pone.0172578>
- [36] Y. R. Tabar and U. Halici, “A novel deep learning approach for classification of eeg motor imagery signals,” *Journal of Neural Engineering*, vol. 14, no. 1, p. 016003, 2017. [Online]. Available: <http://stacks.iop.org/1741-2552/14/i=1/a=016003>
- [37] X. An, D. Kuang, X. Guo, Y. Zhao, and L. He, *A Deep Learning Method for Classification of EEG Data Based on Motor Imagery*. Cham: Springer International Publishing, 2014, pp. 203–210. [Online]. Available: [http://dx.doi.org/10.1007/978-3-319-09330-7\\_25](http://dx.doi.org/10.1007/978-3-319-09330-7_25)
- [38] S. Sakhavi, C. Guan, and S. Yan, “Parallel convolutional-linear neural network for motor imagery classification,” in *2015 23rd European Signal Processing Conference (EUSIPCO)*, Aug 2015, pp. 2736–2740.
- [39] F. Lotte, “Signal Processing Approaches to Minimize or Suppress Calibration Time in Oscillatory Activity-Based Brain-Computer Interfaces,” *Proceedings of the IEEE*, vol. 103, no. 6, pp. 871–890, Jun. 2015.
- [40] R. Fazel-Rezai, B. Z. Allison, C. Guger, E. W. Sellers, S. C. Kleih, and A. Kübler, “P300 brain computer interface: current challenges and emerging trends,” *Frontiers in Neuroengineering*, vol. 5, no. 14, 2012.
- [41] G. Pfurtscheller and C. Neuper, “Motor imagery and direct brain-computer communication,” *Proceedings of the IEEE*, vol. 89, no. 7, pp. 1123–1134, Jul 2001.
- [42] S. Makeig, “Auditory event-related dynamics of the {EEG} spectrum and effects of exposure to tones,” *Electroencephalography and Clinical Neurophysiology*, vol. 86, no. 4, pp. 283 – 293, 1993.
- [43] J. Polich, “Updating p300: An integrative theory of {P3a} and {P3b},” *Clinical Neurophysiology*, vol. 118, no. 10, pp. 2128 – 2148, 2007.

- [44] P. Sajda, E. Pohlmeier, J. Wang, L. C. Parra, C. Christoforou, J. Dmochowski, B. Hanna, C. Bahlmann, M. K. Singh, and S. F. Chang, “In a blink of an eye and a switch of a transistor: Cortically coupled computer vision,” *Proceedings of the IEEE*, vol. 98, no. 3, pp. 462–478, March 2010.
- [45] A. R. Marathe, V. J. Lawhern, D. Wu, D. Slayback, and B. J. Lance, “Improved neural signal classification in a rapid serial visual presentation task using active learning,” *IEEE Transactions on Neural Systems and Rehabilitation Engineering*, vol. 24, no. 3, pp. 333–343, March 2016.
- [46] N. Waytowich, V. Lawhern, A. Bohannon, K. Ball, and B. Lance, “Spectral transfer learning using information geometry for a user-independent brain-computer interface,” *Frontiers in Neuroscience*, vol. 10, p. 430, 2016. [Online]. Available: <http://journal.frontiersin.org/article/10.3389/fnins.2016.00430>
- [47] W. H. R. Miltner, C. H. Braun, and M. G. H. Coles, “Event-related brain potentials following incorrect feedback in a time-estimation task: Evidence for a generic neural system for error detection,” *Journal of Cognitive Neuroscience*, vol. 9, no. 6, pp. 788–798, 1997.
- [48] W. J. Gehring, B. Goss, M. G. H. Coles, D. E. Meyer, and E. Donchin, “A neural system for error detection and compensation,” *Psychological Science*, vol. 4, no. 6, pp. 385–390, 1993. [Online]. Available: <http://pss.sagepub.com/content/4/6/385.abstract>
- [49] M. Falkenstein, J. Hohnsbein, J. Hoormann, and L. Blanke, “Effects of crossmodal divided attention on late {ERP} components. ii. error processing in choice reaction tasks,” *Electroencephalography and Clinical Neurophysiology*, vol. 78, no. 6, pp. 447 – 455, 1991.
- [50] P. Margaux, M. Emmanuel, D. Sébastien, B. Olivier, and M. Jérémie, “Objective and subjective evaluation of online error correction during p300-based spelling,” *Advances in Human-Computer Interaction*, vol. 2012, p. 4, 2012.
- [51] T. O. Zander, C. Kothe, S. Welke, and M. Roetting, *Utilizing Secondary Input from Passive Brain-Computer Interfaces for Enhancing Human-Machine Interaction*. Berlin, Heidelberg: Springer Berlin Heidelberg, 2009, pp. 759–771.
- [52] J. d. R. Milln, R. Rupp, G. Mueller-Putz, R. Murray-Smith, C. Giugliemma, M. Tangermann, C. Vidaurre, F. Cincotti, A. Kubler, R. Leeb, C. Neuper, K. R. Müller, and D. Mattia, “Combining brain-computer interfaces and assistive technologies: State-of-the-art and challenges,” *Frontiers in Neuroscience*, vol. 4, no. 161, 2010.
- [53] M. Spüler, M. Bensch, S. Kleih, W. Rosenstiel, M. Bogdan, and A. Kübler, “Online use of error-related potentials in healthy users and people with severe motor impairment increases performance of a p300-bci,” *Clinical Neurophysiology*, vol. 123, no. 7, pp. 1328 – 1337, 2012.
- [54] D. J. Krusienski, E. W. Sellers, D. J. McFarland, T. M. Vaughan, and J. R. Wolpaw, “Toward enhanced p300 speller performance,” *Journal of neuroscience methods*, vol. 167, no. 1, pp. 15–21, 2008.
- [55] C. Toro, G. Deuschl, R. Thatcher, S. Sato, C. Kufta, and M. Hallett, “Event-related desynchronization and movement-related cortical potentials on the {ECoG} and {EEG},” *Electroencephalography and Clinical Neurophysiology/Evoked Potentials Section*, vol. 93, no. 5, pp. 380 – 389, 1994.
- [56] E. C. Leuthardt, G. Schalk, D. Moran, and J. G. Ojemann, “The emerging world of motor neuroprosthetics: a neurosurgical perspective,” *Neurosurgery*, vol. 59, no. 1, pp. 1–14, 2006.
- [57] S. Gordon, V. Lawhern, A. Passaro, and K. McDowell, “Informed decomposition of electroencephalographic data,” *Journal of Neuroscience Methods*, vol. 256, pp. 41 – 55, 2015.
- [58] G. Pfurtscheller and A. Aranibar, “Event-related cortical desynchronization detected by power measurements of scalp {EEG},” *Electroencephalography and Clinical Neurophysiology*, vol. 42, no. 6, pp. 817 – 826, 1977.
- [59] G. Pfurtscheller and F. L. da Silva, “Event-related eeg/meg synchronization and desynchronization: basic principles,” *Clinical Neurophysiology*, vol. 110, no. 11, pp. 1842 – 1857, 1999.
- [60] K. Liao, R. Xiao, J. Gonzalez, and L. Ding, “Decoding individual finger movements from one hand using human eeg signals,” *PLoS ONE*, vol. 9, no. 1, pp. 1–12, 01 2014.
- [61] N. Bigdely-Shamlo, T. Mullen, C. Kothe, K. M. Su, and K. A. Robbins, “The prep pipeline: Standardized preprocessing for large-scale eeg analysis,” *Frontiers in Neuroinformatics*, vol. 9, no. 16, 2015.
- [62] M. Tangermann, K.-R. Müller, A. Aertsen, N. Birbaumer, C. Braun, C. Brunner, R. Leeb, C. Mehring, K. Müller, G. Mueller-Putz, G. Nolte, G. Pfurtscheller, H. Preissl, G. Schalk, A. Schlögl, C. Vidaurre, S. Waldert, and B. Blankertz, “Review of the bci competition iv,” *Frontiers in Neuroscience*, vol. 6, p. 55, 2012. [Online]. Available: <http://journal.frontiersin.org/article/10.3389/fnins.2012.00055>



- [63] D. Clevert, T. Unterthiner, and S. Hochreiter, “Fast and accurate deep network learning by exponential linear units (elus),” *CoRR*, vol. abs/1511.07289, 2015. [Online]. Available: <http://arxiv.org/abs/1511.07289>
- [64] D. P. Kingma and J. Ba, “Adam: A method for stochastic optimization,” *arXiv*, vol. abs/1412.6980, 2014. [Online]. Available: <http://arxiv.org/abs/1412.6980>
- [65] Theano Development Team, “Theano: A Python framework for fast computation of mathematical expressions,” *arXiv e-prints*, vol. abs/1605.02688, May 2016. [Online]. Available: <http://arxiv.org/abs/1605.02688>
- [66] F. Chollet, “Keras,” <https://github.com/fchollet/keras>, 2015.
- [67] B. Blankertz, R. Tomioka, S. Lemm, M. Kawanabe, and K. r. Muller, “Optimizing spatial filters for robust eeg single-trial analysis,” *IEEE Signal Processing Magazine*, vol. 25, no. 1, pp. 41–56, 2008.
- [68] B. Rivet, A. Souloumiac, V. Attina, and G. Gibert, “xDAWN algorithm to enhance evoked potentials: Application to brain-computer interface,” *IEEE Transactions on Biomedical Engineering*, vol. 56, no. 8, pp. 2035–2043, Aug 2009.
- [69] S. Makeig, A. J. Bell, T.-P. Jung, and T. J. Sejnowski, “Independent component analysis of electroencephalographic data,” *Advances in Neural Information Processing Systems*, pp. 145–151, 1996.
- [70] S. Ioffe and C. Szegedy, “Batch normalization: Accelerating deep network training by reducing internal covariate shift,” *arXiv*, vol. abs/1502.03167, 2015. [Online]. Available: <http://arxiv.org/abs/1502.03167>
- [71] N. Srivastava, G. Hinton, A. Krizhevsky, I. Sutskever, and R. Salakhutdinov, “Dropout: A simple way to prevent neural networks from overfitting,” *Journal of Machine Learning Research*, vol. 15, pp. 1929–1958, 2014. [Online]. Available: <http://jmlr.org/papers/v15/srivastava14a.html>
- [72] Y.-L. Boureau, J. Ponce, and Y. LeCun, “A theoretical analysis of feature pooling in visual recognition,” in *Proceedings of the 27th International Conference on Machine Learning (ICML-10)*, J. Frnkranz and T. Joachims, Eds. Omnipress, 2010, pp. 111–118. [Online]. Available: <http://www.icml2010.org/papers/638.pdf>
- [73] J. T. Springenberg, A. Dosovitskiy, T. Brox, and M. A. Riedmiller, “Striving for simplicity: The all convolutional net,” *arXiv*, vol. abs/1412.6806, 2014. [Online]. Available: <http://arxiv.org/abs/1412.6806>
- [74] A. Barachant, S. Bonnet, M. Congedo, and C. Jutten, “Multiclass Brain-Computer Interface Classification by Riemannian Geometry,” *IEEE Transactions on Biomedical Engineering*, vol. 59, no. 4, pp. 920–928, Apr. 2012.
- [75] A. Barachant and M. Congedo, “A Plug&Play P300 BCI Using Information Geometry,” *arXiv:1409.0107 [cs, stat]*, Aug. 2014, arXiv: 1409.0107. [Online]. Available: <http://arxiv.org/abs/1409.0107>
- [76] K. K. Ang, Z. Y. Chin, C. Wang, C. Guan, and H. Zhang, “Filter bank common spatial pattern algorithm on bci competition iv datasets 2a and 2b,” *Frontiers in Neuroscience*, vol. 6, p. 39, 2012. [Online]. Available: <http://journal.frontiersin.org/article/10.3389/fnins.2012.00039>
- [77] R. Tibor Schirrmester, J. T. Springenberg, L. D. J. Fiederer, M. Glasstetter, K. Eggensperger, M. Tangermann, F. Hutter, W. Burgard, and T. Ball, “Deep learning with convolutional neural networks for brain mapping and decoding of movement-related information from the human EEG,” *ArXiv e-prints*, Mar. 2017.
- [78] Y. Benjamini and D. Yekutieli, “The control of the false discovery rate in multiple testing under dependency,” *The Annals of Statistics*, vol. 29, no. 4, pp. 1165–1188, 2001. [Online]. Available: <http://www.jstor.org/stable/2674075>
- [79] K.-C. Huang, T.-Y. Huang, C.-H. Chuang, J.-T. King, Y.-K. Wang, C.-T. Lin, and T.-P. Jung, “An eeg-based fatigue detection and mitigation system,” *International Journal of Neural Systems*, vol. 26, no. 04, p. 1650018, 2016, pMID: 27121994. [Online]. Available: <http://www.worldscientific.com/doi/abs/10.1142/S0129065716500180>

## 6 Appendix

### 6.1 Effect of Batch Normalization, Dropout and Dense Connections on EEGNet Model Performance

The EEGNet model uses a combination of Batch Normalization [70], Dropout [71] and omitting the traditional dense layer for feature fusion [73]. We systematically evaluated the effect of each of these components by fitting five different architectures and evaluating their performance on four EEG datasets. We fit the EEGNet model with the  $[2, 32] \times [8, 4]$  kernel configuration for this analysis. While we fit each model for 500 epochs, we show only the first 100 for visual clarity. The five models are:

- Model 1: No BatchNormalization, no Dropout and a Dense Layer with 100 units prior to the softmax classification layer.
- Model 2: No BatchNormalization, no Dropout and no Dense Layer.
- Model 3: BatchNormalization, no Dropout and no Dense Layer.
- Model 4: No BatchNormalization, Dropout and no Dense Layer.
- Model 5: BatchNormalization, Dropout and no Dense Layer (the proposed EEGNet model).

A plot of the validation set loss for each dataset, averaged over the 30 folds (9 folds for SMR) is shown in Figure 5. We see that Models 1-3 all start to overfit after only a few epochs. Model 1, which corresponds to the largest model (now having close to 21,000 parameters due to the dense layer) generally has the highest validation loss after 100 epochs. Model 1 also exhibits unusual behavior in MRCP and SMR at around the 70-80 epoch range. Models 2, which is much smaller than Model 1 due to having no Dense layer, still overfits after only a few epochs, suggesting more regularization is needed. Model 3, which incorporates Batch Normalization, also exhibits a linear increase in validation loss after a few epochs, although the rate of increase is slightly lower than Models 1 and 2. A common feature of Models 1-3 is that they all lack Dropout, which has proven effective in discouraging overfitting in many previous works. Models that do contain Dropout (Models 4-5) effectively counter overfitting; BatchNormalization together with Dropout has a small but noticeable effect on the validation loss.

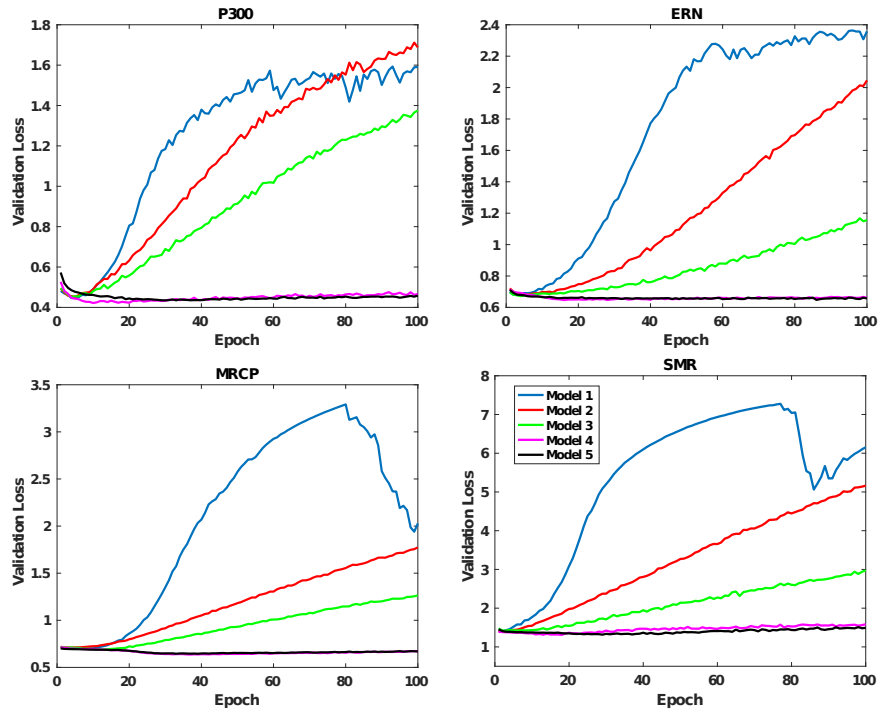


Figure 5: Validation Loss of five different models, each with different combinations of Batch Normalization, Dropout and a Dense Layer with 100 hidden units. Models 1-3, which do not have Dropout, all start to overfit within the first few epochs. Models 4 and 5, which do contain Dropout, effectively counter overfitting. Batch Normalization provides a small but noticeable improvement in validation loss.